ISSN 2228-9860 eISSN 1906-9642 CODEN: ITJEA8

International Transaction Journal of Engineering, Management, & Applied Sciences & Technologies

http://TuEngr.com

The Effect of Impedance Stiffness Parameter on Grasping Force for Different Object Textures

Muhammad Shahmir Selamat[1], Ruhizan Liza Ahmad Shauri[1*], Ahmad Badiuzzaman Roslan[1]

[1]*School of Electrical Engineering, College of Engineering, Universiti Teknologi MARA, 40450 Shah Alam, Selangor, MALAYSIA.*

**Corresponding Author (Tel: +60125002912, Email: ruhizan @uitm.edu.my).*

Paper ID: 15A4D

Volume 15 Issue 4

Received 23 May 2023
Received in revised form 24 March 2024
Accepted 04 May 2024
Available online 02 July 2024

Keywords:
Three-fingered robot hand; Grasping force; Impedance control; Stiffness parameter; Object texture; Robot hand system; Force control.

Abstract

Upon developing an intelligent method for a robot to vary impedance stiffness parameters by itself, the relationship between varied stiffness parameters, measured force and object texture needs to be obtained. A three-fingered robot hand was tested for real grasping on a bottle and a ball that represent a harder and softer object texture, respectively. Varying the parameter at 1000, 500, and 250 for each object, the experiment used a 6-axis force-torque sensor to measure the force for analysis. The stiffness at 1000 showed the most significant difference in force rate compared to the other values for both objects. Besides, at this stiffness, the bottle grasping has recorded 84% of force rate value measured in the range of 0 to 0.6 and 40% in 0.21 to 0.4. Comparatively, the force rate data are most frequently measured by 48% in the range of 0 to 0.2 for ball grasping with the same stiffness. Moreover, from the most frequent range of the force rate, the average value for a bottle is found higher than the ball. These show that object texture is a feasible parameter to be used for developing the object recognition method based on force data in the future.

Disciplinary: Electrical Engineering (Robotics, Systems and Control).

Cite This Article:

Selamat M.S., Shauri R.L.A., Roslan A.B. (2024). The Effect of Impedance Stiffness Parameter on Grasping Force for Different Object Textures. *International Transaction Journal of Engineering, Management, & Applied Sciences & Technologies, 15*(4), 15A4D, 1-12. http://TUENGR.COM/V15/15A4D.pdf DOI: 10.14456/ITJEMAST.2022.23

1 Introduction

The robotic hand is one of the end effector types that needs to be programmed for delicate control in executing object manipulation tasks. In this modern era, there are various types of robot hands built to assist humans whether for industrial use or for human daily life. However, in the manufacturing industry for instance, robot tasks that involve grinding or deburring require steady force to be applied by the robot and its ability to reject high-frequency disturbances to produce quality results (Anderson and Spong, 1988). The limitations of the robot hand might be caused by the nonlinear disturbances from the joints' elastic gear, shaft windup, or friction in the gears. Thus, in order to make a perfect object manipulation, a human-like robotic hand needs not only be artificially intelligent but also have the sense of touch and control. In bringing up this feature, the impedance control method is one of the ways to control the exerted force that can be measured by an appropriate sensor embedded in the robotic hand.

Impedance control is a dynamic control approach that produces the required motion of mechanical hardware related to the force measured from its interaction with the environment. Based on the interactive force, the appropriate position of the equipment could be modified to avoid excessive force applied by the hardware during the manipulation. According to (Spong, 1989), impedance control can be applied to the inner or outer loop control of a system where applying it in the former will make it a nonlinear control and for the latter as a linear control for the system.

A bimanual arm/hand system which consists of four fingers on each arm each has applied an impedance controller for grasping an object (Caccavale et al., 2013). Their simulations showed that the control counteracted the position and force errors effectively when reaching its steady state form of the step response. In a study on mimetic communication of physical human-robot interaction (pHRi) using an IRT humanoid robot, impedance control was integrated into the controller to perform human-robot interaction tasks, which require physical contact between humans and robots. The movement of this robot is controlled by using marker tracking and data from human motions and the application of impedance control proved to be capable of providing safe and smooth contact with humans (Lee et al., 2009).

Force-torque sensor integration in industrial robot control has been done by Loske using KR 16-2 industrial robot with KRC 2 control from KUKA GmbH. The exerted force onto the object was measured by the Schunk force-torque sensor (model SI -13 -10) and easily visualized by the measurement system in a 3D coordinate system for analysis (Loske & Biesenbach, 2014). A different type of force/torque sensors were used to monitor the work by an end-effector of an industrial robot in handling work pieces. The sensor has the capability of measuring each force and moment in three direction axes, which means providing rich and accurate data on force-torque data for robot control (Alpek et al., 2002).

Wei et al. stated that their proposed impedance control self-tuning strategy has made the contact force follow the desired input more efficiently compared to the traditional impedance control which has fixed values of the control parameters (Wei et al., 2020). To realize the natural feeling of control to be applied to their robot hand, Tsuji et al. have implemented an experiment to determine the impedance parameter of the human hand using the least square method (Tsuji et al., 2010). In another study, an experiment on position and impedance control of a multi-finger tendon-driven robotic hand was done (Sainul et al., 2016). The results showed that the proposed impedance control law method achieved the desired angle faster compared to a position control law method due to the advantage of controlling the force sensed by the robot system. A new force impedance controller was suggested by (Almeida et al., 1999) where the method can operate in two modes; as a force-limited impedance controller or a position-limited force controller. The former is used when the force reference is not set but a force reference will be used to limit the applied force by the manipulator when excessive force is measured. On the other hand, the latter will be used when a force reference can be obtained but a position reference will be used to limit the position when position error occurs.

Jo et al. (2013) presented a grasping force control of a robotic hand based on torque velocity transformation using a force/torque (F/T) sensor. The result showed that the measured force followed the desired force without high force overshoot. Hanafusa and Hunang have proposed a position-based impedance control where the external force and the displacement of the PUMA's hand position were modelled as the mass-spring viscous system (Hanafusa & Hunang, 2018). The moment and the force exerted on the hand were fed back to the impedance model blocks to correct the displacement and posture reference for the robot.

Consequently, having interactive forces to be measured when robots do their work, several object classification studies have been implemented by previous researchers. An intelligent classification method developed using a Bayesian algorithm (Fischel and Loeb, 2012) was used to recognize grasped objects using Shadow Hand by exploration of the finger over the object surface (Xu et al., 2013). The multimodal tactile BioTac sensor which is capable of measuring the pressure, vibration, and temperature was used to identify the compliance of contact, vibration, and thermal conductivity when the robot executed six exploratory movements on the objects. Using the same robot hand and a similar method, a solution for object recognition based on an object's surface texture properties was introduced (Kaboli et al., 2015). The Shadow Hand robot hand was attached with an artificial skin on the fingertips with the same BioTac sensors attached on each fingertip to collect two types of tactile data which are measured by the pressure sensors and impedance sensing electrode arrays. To collect the grasping data for object recognition, the robot hand was programmed to hold the objects for 2 seconds, which was then repeated 10 times. During the grasp, the thumb and index fingers slide over the object surface for 2 seconds and repeat 20 times for each object. Support Vector Machine (SVM) was then used to develop the learning model for object recognition based on the collected raw data. As a result, the robot hand was able to classify the object by texture properties with 97% recognition accuracy. The tactile data were used once again to discriminate in-hand objects via texture properties using the online transfer learning method where the work improved the recognition accuracy performance to 97% - 100% with lesser training samples (Kaboli et al., 2016) and they had improved more to a more robust learning algorithm with tactile descriptors that can classify objects without limitations on the number of the tactile sensors, sensing technologies, type of exploratory movements, and duration of the objects' surface exploration (Kaboli and Cheng, 2018).

Konstantinova et al. (2017) developed a flexible hybrid fiber optical force/proximity sensor to measure the normal and lateral force signals when a robot's fingertip makes contact with objects. Estimation of the grasping object position is initially made by using a proximity sensor that calculates the distance between the finger and the object. The measured force and proximity data were used for classification by the Support Vector Machine (SVM) method to differentiate the object's stiffness which is between hard and soft textures. Without having the knowledge on a set of household objects, the method achieved an 87% of classification accuracy, thus proving the feasibility of the sensor for the required measurement.

Another object recognition study has been done on an Allegro Hand (Funabashi et al., 2018). Twenty different objects were selected for testing where ten consists of easily distinguishable objects while another ten are objects which are similar to bottle shape. The robot hand was embedded with a previously developed uSkin tactile sensor which provides widely distributed force vector sensors covering all phalanges of the four fingers of the robot hand. Three types of neural network algorithms were tested for object recognition i.e. a simple feedforward, Recurrent Neural Network (RNN), Convolutional Neural Network (CNN). The recognition results showed that CNN outperformed the other two with 95% recognition accuracy for 20 test objects.

In this study, the force control study continues from the previous three-fingered robotic hand developed by Jaafar and Shauri (2013). A position-based impedance control which takes the feedback inputs from a two-axis force measurement was implemented to correct the displacement reference of the joints (Nasir et al., 2018). Prior to selecting the impedance control parameters, the effect of varying the parameters was investigated and the results showed that the impedance stiffness has been the most influential parameter (Nasir, 2017). Consequently, the control method was modified to use a new 6-axis force torque (F/T) sensor which has been proven feasible in simulation tests (Shauri et al., 2020). However, in order to grasp different textures of objects, the robot hand needs to adjust the stiffness of the joints by determining the suitable stiffness parameter value by itself using an intelligent method. Prior to the development of the intelligent recognition method like in the above-cited research, in this work, an analysis of real grasping data for observing the effect of different impedance stiffness parameter values on the measured force when grasping different objects is implemented. The experimental results and observations from this study are vital and later will be beneficial inputs to the development of the recognition algorithm for the hand in the future.

2 Robot Hand System and Impedance Control Parameter

2.1 Position-Based Impedance Control

The position-based impedance control as illustrated in Figure 1 was developed by considering the translational impedance equation to enforce an equivalent mass-spring-dashpot behaviour for the position displacement of the fingertip. It starts by setting the force reference, F_{ref} to a desired value. When the robot's fingertip is in contact with an object or an environment, external force F_{ext} will be produced. In this work, F_{ext} was taken from finger 1 only as it is the finger controlled by the impedance method whereas the movement of the other fingers is short-circuited to follow the same trajectory of finger 1. When F_{ext} exceeds F_{ref}, the position-based impedance control will be activated and it will modify the desired tip-end position, P_d to P_{dnew} by using the impedance dynamics equations (1) and (2) (Shauri et al., 2020). *Md, Dd* and *Kd* are the impedance parameters known as mass, damping, and stiffness coefficients where in this work only *Kd* is varied. These coefficients can produce the softness of the robot's hand by changing the tip-end position based on the forces exerted on the robot's fingers. In the case where no force interaction occurs at the fingertip of the robot hand, P_d will be equal to P_{dnew}.

$$F_{ext} - F_{ref} = M_d(\Delta\ddot{P}) + D_d(\Delta\dot{P}) + K_d(\Delta P) \quad (1),$$

$$\Delta P = P_{dnew} - P_d \quad (2).$$

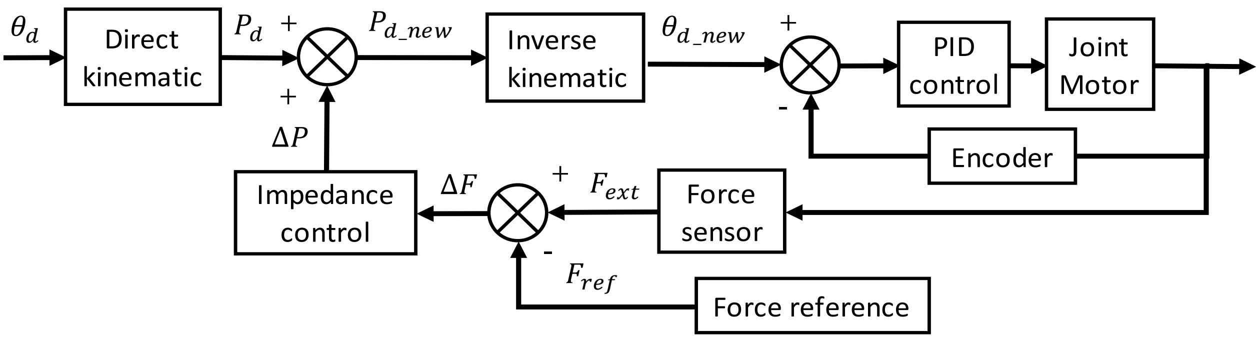

Figure 1: Position-Based Impedance Control (Nasir et al., 2018).

2.2 Robot Hand System

The robot hand as shown in Figure 2 consists of one palm and three fingers. It is made of seven DOF joints where each joint represents 1 DOF. Each joint of the fingers is driven by a DC-Micro motor equipped with encoders to measure the motor position. A 6-axis F/T sensor (ATI NANO17) is placed at the fingertip of the hand for the force measurement in the x, y, and z directions. The modified control algorithm based on the new sensor and the interface applying multiple PCIs proposed by Shauri et al. (2020) were used in this work.

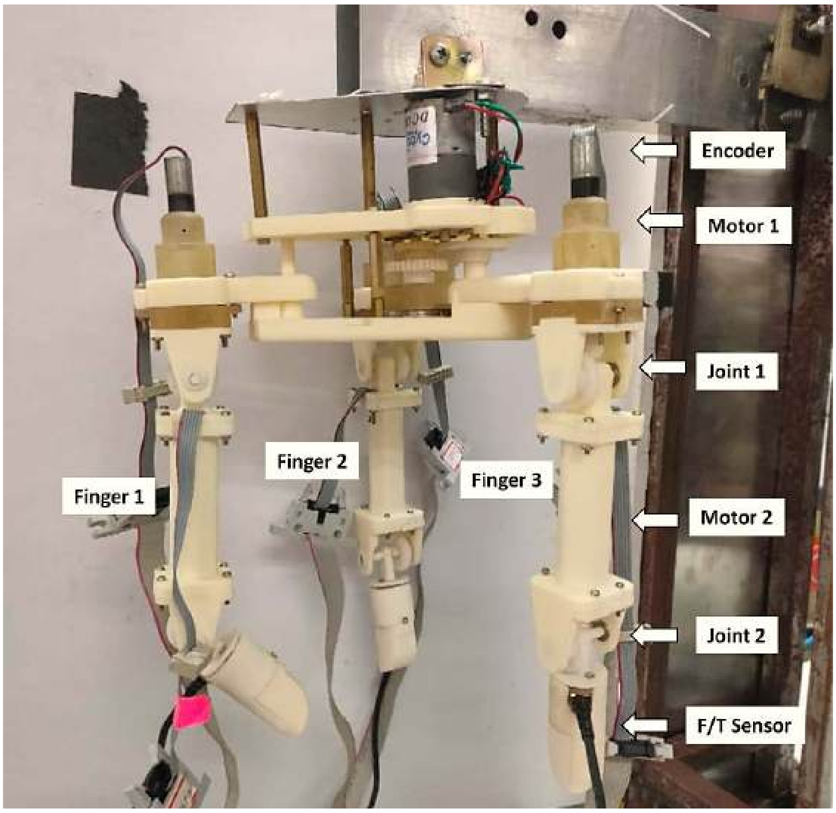

Figure 2: Three-fingered Robot Hand (Shauri et al., 2020).

3 Methodology

The new application by Shauri et al. (2020) gave a more accurate force measurement compared to the previous application by Nasir et al. (2018). However, the robot hand was not yet tested for real object grasping which may have different textures. Handling such objects requires adjustment of the impedance parameter based on the amount of external forces exerted onto the robot's fingertip.

3.1 Description of Grasping Data Collection

In this work, the three-fingered robot hand is tested for real grasping of objects with different textures i.e. a harder plastic bottle and a softer spongy ball. Here, while varying *Kd* to 250, 500, and 1000, the external force signal measured by the F/T sensor placed on finger 1 was collected for analysis.

The grasping data have been collected in a separate study using the experimental setup as shown in Figure 3. A combination of multiple PCI has been used to establish the interface between the hardware and software. The position-based impedance control in Figure 1 was implemented on Real-time Windows Target in Matlab Simulink.

In the experiment, *Kd*, *Md* and *Dd* were initially set to 1000, 1, and 10, respectively. The force reference F_{ref} was set at a relatively small value of 0.1N. The finger joints were moved to the grasping position as shown in Figure 4 where joint 1 J1 was directed to 10° while joint 2 J2 was directed to 33°. The external force namely F_{ext0} was collected at 0.25s after the finger touched the object and the force was once again collected as F_{ext1} as the grasping tightened at 1s. Next, the grasping force rate F_{rate} is calculated using both F_{ext0} and F_{ext1} as written in (3). Then, the grasping steps were repeated for each object with varied Kd = 500 and Kd = 250.

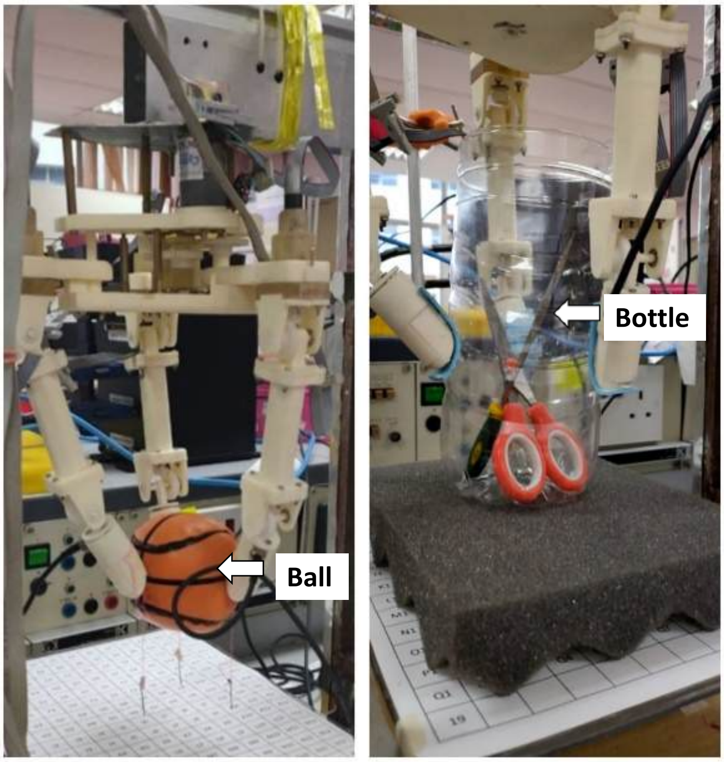

Figure 3: Data collection setup of the three-fingered robot hand.

The experiments that have been implemented faced several difficulties with the hardware nonlinearities that came from the friction and elasticity of the gears (made of plastic), loose connections of the joint components and the backlash of the gears, especially after several executions of the grasping experiments. These have somehow affected the time and cost of the data collection experiments when the hand failed the grasp. Finally, after confirming the hardware to be in good condition, 25 sets of F_{rate} data for each of the bottle and ball cases have successfully been collected for analysis.

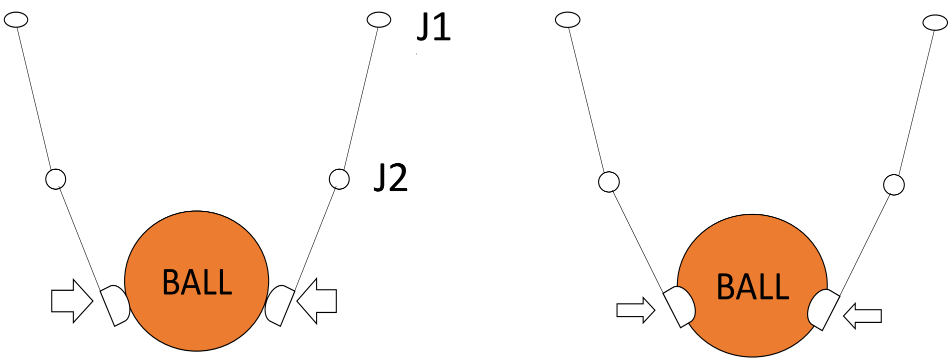

Figure 4: Position of the fingertip of the three-fingered robot hand

$$F_{rate} = \frac{F_{ext1} - F_{ext0}}{1 - 0.25} \quad (3).$$

3.2 Analysis method

There are a few methods in data preprocessing which include data cleaning, data integration, data transformation, and data reduction. In this work, the data transformation which is the normalization technique was used to analyze the effect of varying impedance stiffness parameters on the grasping of different object textures.

Normalization is the process of scaling data attributes of different scales to be within a narrower range which is typically from 0 to 1. A nonlinear system used in this work requires the normalization of the collected data for fair and comparable analysis relative to the standard scale. The normalization of each F_{rate} or x is written in (4). x_{min} and x_{max} are the minimum and the maximum value of F_{rate}, respectively.

$$X_{normalize} = \frac{x - x_{min}}{x_{max} - x_{min}} \quad (4).$$

One of the most common ways of displaying frequency distributions of data is by using a histogram graph. A frequency distribution graph can show how frequently each value in the data appears across the variable's range. Here, F_{rate} data were normalized between 0 and 1, and the results were displayed on a histogram graph to observe the behaviour of F_{rate} related to the varied parameters i.e. *Kd* and the object texture.

4 Result and Discussion

From Figure 5(a) and Figure 5(c), in the case of bottle grasped with *Kd* set to 250 and 500 experiments, the frequency of F_{rate} measured is quite evenly distributed across the different ranges. In other words, the frequency of F_{rate} with these *Kd* to be measured significantly in a range of values could not be determined as compared to the data for *Kd* of 1000 as shown in Figure 5(e) which recorded 84% of force rate value measured in the range of 0 to 0.6. Within this range, the force rate value was mostly in the range of 0.21 to 0.4 or 40% of the total number of experiments.

On the other hand, from the grasping data for a softer spongy ball in Figure 5(b) and Figure 5(d), F_{rate} is frequently measured in the range value of 0 to 0.4 when setting *Kd* at 250 and 500. However, it can be observed that F_{rate} is significantly measured by 48% in one class range i.e. within 0 to 0.2 F_{rate} value for *Kd* 1000, as shown in Figure 5(f).

From the above results, it can be concluded from both bottle and ball cases that the stiffness parameter at 1000 showed the most significant difference of F_{rate}. In other words, higher *Kd* means higher stiffness of the robot finger and therefore makes the robot finger less flexible to grasp objects with harder texture. Besides, at the same stiffness, the F_{rate} data are found to be most frequent in the range of 0 to 0.2 for a ball, and 0.21 to 0.4 for a bottle which means that grasping a bottle produces higher force measured in a specific time compared to grasping the softer ball. This is also can be proven based on the most frequent range of force rate where the average value of force rate for a bottle is higher than the ball. Figure 6 graphed the F_{rate} from all 25 sets of data for both objects.

Next, the calculations of the minimum, maximum and standard deviation of F_{rate} values are shown in Figure 7. It can be observed that F_{rate} for Kd = 1000 in the ball case gives the smallest standard deviation and is moderately small for a bottle. A smaller standard deviation indicates that the data is clustered around the mean value of the respective F_{rate}. Besides, the average F_{rate} for the bottle on any Kd values is comparatively higher than for the ball, which means that F_{rate} tends to be higher for bottle cases.

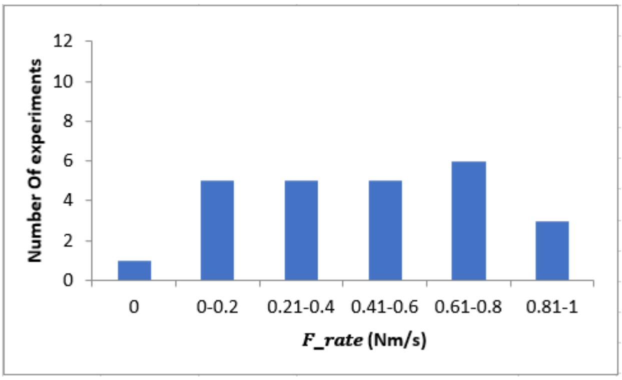

(a) Bottle F_{rate} data for Kd = 250

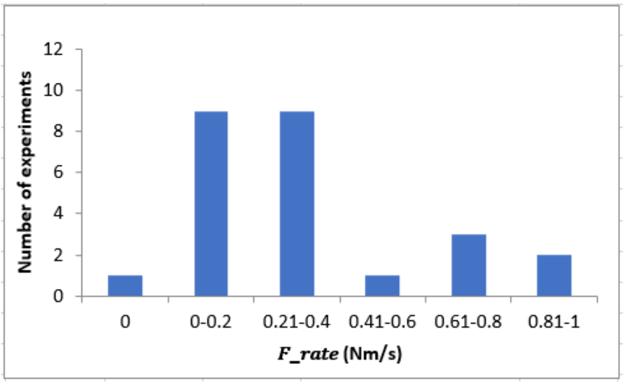

(b) Ball F_{rate} data for Kd = 250

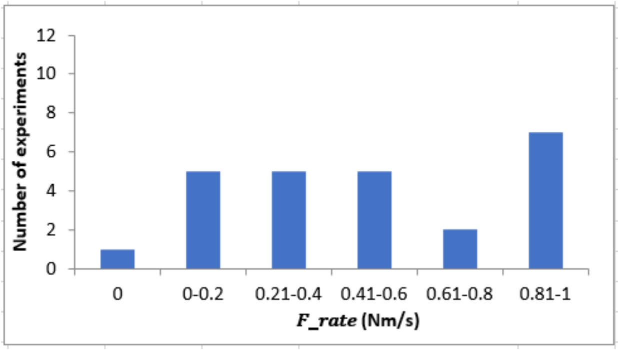

(c) Bottle F_{rate} data for Kd = 500

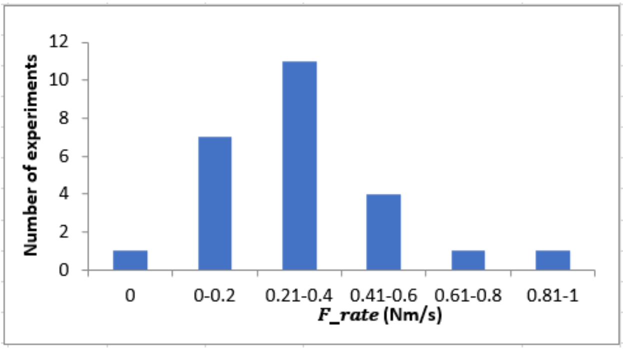

(d) Ball F_{rate} data for Kd = 500

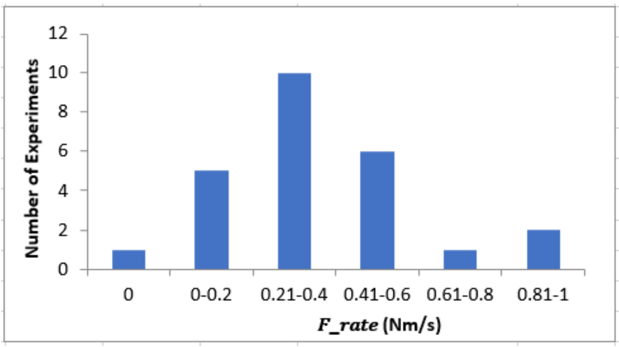

(e) Bottle F_{rate} data for Kd = 1000

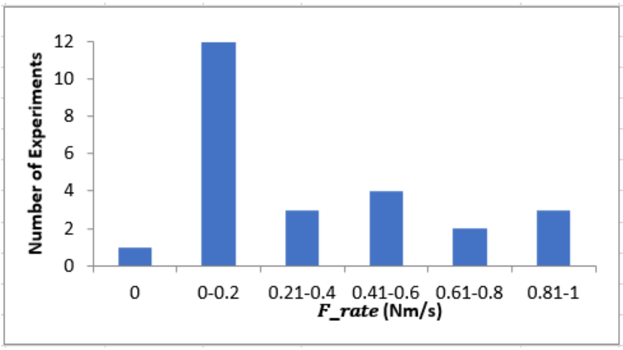

(f) Ball F_{rate} data for Kd = 1000

Figure 5: Distribution of F_{rate} after normalization.

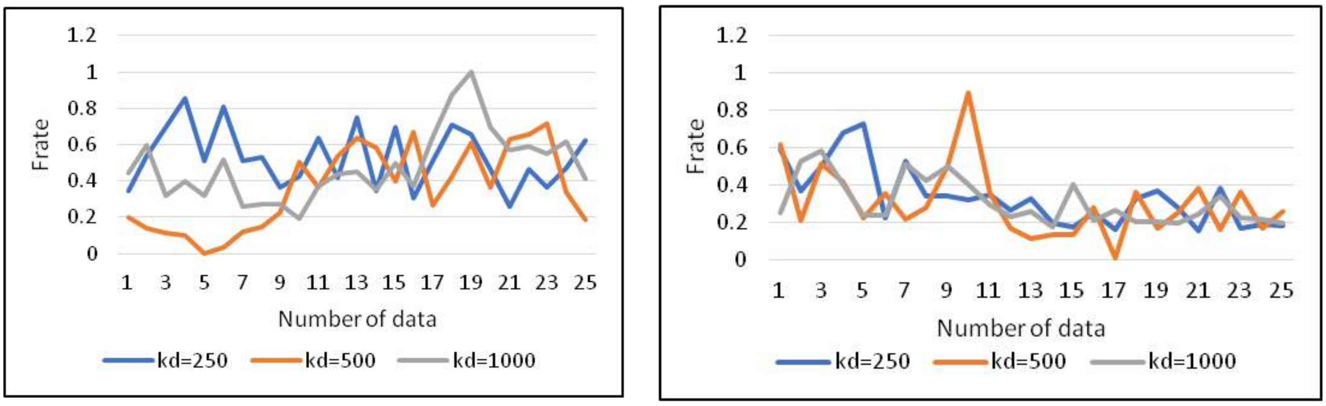

(a) F_{rate} of grasping a bottle (b) F_{rate} of grasping a ball

Figure 6: F_{rate} for different object textures.

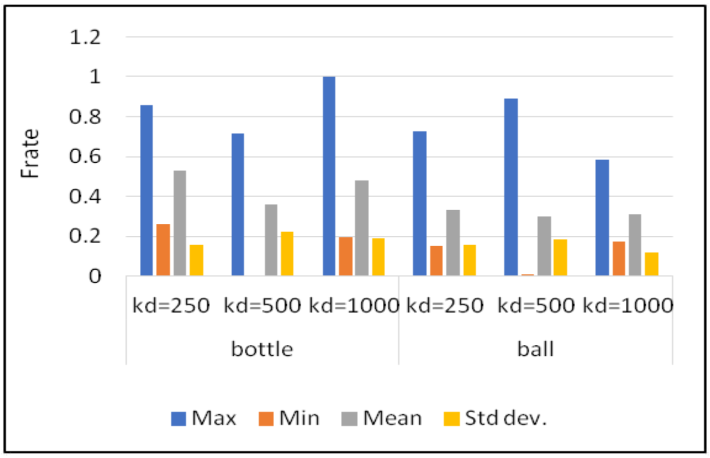

Figure 7: Maximum, minimum, mean, and standard deviation of F_{rate}.

5 Conclusion

In order to grasp different textures of objects, a robot hand needs to be able to adjust the stiffness of the joints by determining the suitable stiffness parameter value by itself using an intelligent method. Prior to the development of the intelligent recognition method, in this work, the effect of varying impedance stiffness parameter *Kd* on the measured force when grasping objects with different textures has been observed. The grasping experiments were executed in a separate work using a three-fingered robotic hand that was developed with position-based impedance control in previous studies. From the analysis results, *Kd* = 1000 showed the most significant difference in force rate for the two objects compared to the other stiffness values. Besides, at the same stiffness, the F_{rate} data are mostly measured in the range of 0 to 0.2 for a ball compared to the higher range of 0.21 to 0.4 for a bottle, by 48% and 40% from the total number of experiments, respectively.

Based on the most frequent range of the force rate measured, the average value of the force rate for a bottle is higher than the ball. It can also be concluded that force rate is applicable to be used as the parameter for determining object texture for grasping tasks by the robot hand. The observations from this work are vital and will be a beneficial input to the development of the intelligent recognition algorithm for the hand in the future.

6 Availability of Data and Material

Data can be made available by contacting the corresponding author.

7 Acknowledgement

This research is supported by FRGS (600-IRMI/FRGS 5/3 (326/2019) grant. The authors acknowledged the Ministry of Higher Education (MOHE) for the approved fund and to the College of Engineering, Universiti Teknologi MARA for providing the laboratory space and equipment.

8 References

Almeida, F., Lopes, A., & Abreu, P. (1999). Force-impedance control: a new control strategy of robotic manipulators. Recent advances in Mechatronics, 1, 126-137.

Alpek, F., Kovacs, S., Krys, N., & Terbuc, M. (2002). Multi-sensor systems based on force/torque/pressure sensors for monitoring of grippers. In Proceedings of International Workshop on Advanced Motion Control (AMC), 551–555. https://doi.org/10.1109/amc.2002.1026980.

Anderson, R. J., & Spong, M. W. (1988). Hybrid impedance control of robotic manipulators. *IEEE Journal on Robotics and Automation*, *4*(5), 549-556.

Caccavale, F., Muscio, G., & Pierri, F. (2013). Grasp force and object impedance control for arm/hand systems. In Proceedings of 16th International Conference on Advanced Robotics (ICAR 2013), 1. https://doi.org/10.1109/ICAR.2013.6766458.

Fishel, A.J. and Loeb, G.E., Bayesian exploration for intelligent identification of textures, Frontiers in Neurorobotics, vol. 6, no. 4, 1-20.

Funabashi, S., Morikuni, S., Geier, A., Schmitz, A., Ogasa, S., Torno, T. P., Somlor, S., & Sugano, S. (2018). Object Recognition Through Active Sensing Using a Multi-Fingered Robot Hand with 3D Tactile Sensors. In Proceedings of IEEE International Conference on Intelligent Robots and Systems, 2589–2595. https://doi.org/10.1109/IROS.2018.8594159.

Hanafusa, T., & Hunang, Q. (2018). Control of position, attitude, force and moment of 6-DOF manipulator by impedance control. In Proceedings of 2018 15th International Conference on Control, Automation, Robotics and Vision (ICARCV 2018), 1, 274–279.

Jaafar, J., & Shauri, R.L.A. (2013). Three-fingered robot hand for assembly works. In Proceedings of 2013 IEEE 3rd International Conference on System Engineering and Technology, ICSET 2013, 237–241.

Jo, J., Kim, S.K., Oh, Y., & Oh, S.R. (2013). Grasping force control of a robotic hand based on a torque-velocity transformation using F/T sensors with gravity compensation. In Proceedings of Industrial Electronics Conference, 4150–4155.

Kaboli, M., De La Rosa, A.T., Walker, R., & Cheng, G. (2015). In-hand object recognition via texture properties with robotic hands, artificial skin, and novel tactile descriptors. In Proceedings of IEEE-RAS International Conference on Humanoid Robots, 1155–1160. https://doi.org/10.1109/HUMANOIDS.2015.7363508.

Kaboli, M., Walker, R., & Cheng, G. (2016). Re-using prior tactile experience by robotic hands to discriminate in-hand objects via texture properties. In Proceedings of IEEE International Conference on Robotics and Automation, 2242–2247. https://doi.org/10.1109/ICRA.2016.7487372.

Kaboli, M. and Cheng, G. (2018). Robust Tactile Descriptors for Discriminating Objects from Textural Properties via Artificial Robotic Skin, IEEE Transactions on Robotics, vol. 34, no. 4, pp. 985-1003.

Konstantinova, J., Cotugno, G., Stilli, A., Noh, Y., & Althoefer, K. (2017). Object classification using hybrid fiber optical force/proximity sensor. In Proceedings of IEEE Sensors, 2017-Decem, 1–3. https://doi.org/10.1109/ICSENS.2017.8234057.

Lee, D., Ott, C., & Nakamura, Y. (2009). Mimetic communication with impedance control for physical human-robot interaction. In Proceedings of IEEE International Conference on Robotics and Automation, 1535–1542. https://doi.org/10.1109/ROBOT.2009.5152857.

Nasir, K., Shauri, R.L.A., Salleh, N.M., Remeli, N.H. (2017). Effect of Varying Impedance Parameters for Position-based Impedance Control of a Three-fingered Robot Hand. Pertanika Journal of Science & Technology, 25(S), 111-112.

Nasir, K., Shauri, R. L. A., Salleh, N. M., & Remeli, N. H. (2018). Implementation of two-axis position-based impedance control with inverse kinematics solution for A 2-DOF robotic finger. International Journal of Engineering and Technology(UAE), 7(3), 10–14.

Sainul, I., Deb, A.K., & Deb, S. (2016). Position and Impedance Control of a Multi-Finger Tendon-Driven Robotic. In Proceedings of 6th International and 27th All India Manufacturing Technology, Design and Research Conference (AIMTDR-2016).

Shauri, R.L.A., Roslan, A.B., & Zarib, Z.S.M. (2020). Application of 6-axis force torque (F/T) sensor for a three fingered robot hand impedance control. In Proceedings of 2020 IEEE 10th International Conference on System Engineering and Technology, ICSET 2020, 262–266.

Spong, M.W. (1989). On the force control problem for flexible joint manipulators, IEEE Transactions on Automatic Control, vol. 34, no. 1, 107-111.

Tsuji, T., Shima, K., Bu, N., & Fukuda, O. (2010). Biomimetic Impedance Control of an EMG-Based Robotic Hand. 213–231. Robot Manipulators Trends and Development. IntechOpen Book Series.10.5772/9184.

Wei, J., Yi, D., Bo, X., Guangyu, C., & Dean, Z. (2020). Adaptive Variable Parameter Impedance Control for Apple Harvesting Robot Compliant Picking. Complexity, 1-15.

Xu, D., Loeb, G.E., and Fishel, A.J., Tactile identification of objects using bayesian exploration. In Proceedings of 2013 IEEE International Conference on Robotics and Automation, 3056–3061.

Muhammad Shahmir Selamat has recently obtained his Bachelor of Engineering (Hons) in Electronics Engineering from the School of Electrical Engineering, College of Engineering, Universiti Teknologi MARA. His interest involves Automation, Robotics and Process Control.

Ahmad Badiuzzaman Roslan is a postgraduate student of Master of Science in Electrical Engineering at the School of Electrical Engineering, College of Engineering, Universiti Teknologi MARA. He obtained his Bachelor of Engineering (Hons) in Electronics Engineering from the same university. His interest involves Artificial Intelligence (AI), Control Systems, and Audio Processing.

Dr. Ruhizan Liza Ahmad Shauri is a Lecturer in System Engineering Studies, at the School of Electrical Engineering, College of Engineering, Universiti Teknologi MARA. She obtained his PhD degree from the University of Chiba, Japan in Systems Artificial Science under the Faculty of Mechanical Engineering. Her research focuses on robotic design, control systems, and image processing.